Characterization of overall ceramide species in human *stratum corneum*[S]

Yoshinori Masukawa,[1] Hirofumi Narita, Eri Shimizu, Naoki Kondo, Yoshiya Sugai, Tsuyoshi Oba, Rika Homma, Junko Ishikawa, Yutaka Takagi, Takashi Kitahara, Yoshinori Takema, and Katsumi Kita

Tochigi Research Laboratories, Kao Corporation, Ichikai, Haga, Tochigi 321-3497, Japan

Abstract Ceramides (CERs) in human *stratum corneum* (SC) play physicochemical roles in determining barrier and water-holding functions of the skin, and specific species might be closely related to the regulation of keratinization, together with other CER-related lipids. Structures of those diverse CER species, however, have not been comprehensively revealed. The aim of this study was to characterize overall CER species in the SC. First, we constructed 3D multi-mass chromatograms of the overall CER species, based on normal-phase liquid chromatography (NPLC) connected to electrospray ionization-mass spectrometry (ESI-MS) using a gradient elution system and a postcolumn addition of a volatile salt-containing polar solvent. The CERs targeted from the 3D chromatograms were structurally analyzed using NPLC-ESI-tandem mass spectrometry (MS/MS), which resulted in the identification of 342 CER species in the inner forearm SC.[Jlr] This led to the discovery of a new CER class consisting of α-hydroxy fatty acid and dihydrosphingosine moieties, in addition to the 10 classes generally known. The results also revealed that those CERs contain long-chain (more than C_{18})-containing sphingoids and a great number of isobaric species. These novel results will contribute not only to physiochemical research on CERs in the SC but also to lipidomics approaches to CERs in the skin.—Masukawa, Y., H. Narita, E. Shimizu, N. Kondo, Y. Sugai, T. Oba, R. Homma, J. Ishikawa, Y. Takagi, T. Kitahara, Y. Takema, and K. Kita. **Characterization of overall ceramide species in human *stratum corneum*. *J. Lipid Res.* 2008. 49: 1466–1476.**

Ceramides (CERs) not only have physicochemical roles as a barrier against cell permeability and as a matrix for the association of membrane proteins but also have physiological roles in signal transduction and cell regulation relevant to apoptosis, cell growth arrest, differentiation, senescence, and immune responses (1–4). Compared with other human cells/tissues, the *stratum corneum* (SC) of human skin has extremely complex CERs consisting of fatty acid moieties (nonhydroxy, α-hydroxy, or ester-linked ω-hydroxy) and sphingoid moieties (sphingosine, dihydrosphingosine, phytosphingosine, or 6-hydroxy-sphingosine) (5). CERs in human SC contribute to the formation of lamellae structures at intercellular spaces among the horny cells in the SC together with cholesterol and free fatty acids and play important physicochemical roles in determining cutaneous barrier and water-holding functions (6–9). On the other hand, some scientists are interested in the dynamics of CER-related lipids in differentiated keratinocytes, where apoptosis occurs in the skin (10). In recent years, the possibility that specific CER species may be involved with human diseases and/or with physiological phenomena has also been proposed (11–13). This suggests that specific CER species might be closely related to the regulation of keratinization from living epidermal cells to dead horny cells, together with other CER-related lipids. However, until now, structures of CER species present in the SC have not been comprehensively revealed.

For human cells/tissues, except for hair and SC, there are 3 classes (combinations of nonhydroxy fatty acids and sphingosines, nonhydroxy fatty acids and dihydrosphingosines, and α-hydroxy fatty acids and sphingosines) that contain simple species with combinations of C_{18}-containing sphingosines or dihydrosphingosines and even carbon-containing nonhydroxy or α-hydroxy fatty acids (13–15). Human hair CERs are more complex than are those in human cells/tissues, because hair contains 4 classes (combinations of nonhydroxy fatty acids and sphingosines, nonhydroxy fatty acids and dihydrosphingosines, α-hydroxy fatty acids and sphingosines, and α-hydroxy fatty acids and dihydrosphingosines), and the predominant class, CERs consisting of nonhydroxy fatty acid and dihydrosphingosine moieties,

Abbreviations: CER, ceramide; ESI-MS, electrospray ionization-mass spectrometry; MS/MS, tandem mass spectrometry; NPLC, normal-phase liquid chromatography; SC, *stratum corneum*; TIC, total ion chromatogram.
[1] To whom correspondence should be addressed.
e-mail: masukawa.yoshinori@kao.co.jp
[S] The online version of this article (available at http://www.jlr.org) contains supplementary data in the form of two figures and two tables.

has C_{16}-, C_{17}-, C_{18}-, C_{19}-, or C_{20}-containing dihydrosphingosines and not only even but also odd carbon-containing nonhydroxy fatty acids (16). On the other hand, human SC has even more-complex CERs. Thus, from earlier days when CERs were analyzed using TLC, it was recognized that in the SC there are 7 CER classes corresponding to seven spots on the TLC plates (17, 18). Robson et al. (5) and Vietzke et al. (19) demonstrated that the seven spots correspond to 9 CER classes, because five of the spots come from single CER classes (combinations of nonhydroxy fatty acids and phytosphingosines, nonhydroxy fatty acids and 6-hydroxy-sphingosines, α-hydroxy fatty acids and phytosphingosines, α-hydroxy fatty acids and 6-hydroxy-sphingosines, and ester-linked ω-hydroxy fatty acids and sphingosines), whereas two spots contain 2 CER classes (combinations of nonhydroxy fatty acids and dihydrosphingosines, nonhydroxy fatty acids and sphingosines, α-hydroxy fatty acids and sphingosines, and ester-linked ω-hydroxy fatty acids and 6-hydroxy-sphingosines). After that, an additional class, CERs consisting of ω-hydroxy fatty acid and phytosphingosine moieties, was discovered (20), which seemed to have been not recognized earlier due to its trace levels in the SC. Therefore, in addition to the 2 classes of covalently bound types (5, 21), 10 classes have been known as free extractable types in the SC. A few reports have described combinations of fatty acid and sphingoid moieties in CER species in the SC, such as those by Vietzke et al. (19) and Farwanah et al. (22). However, those descriptions were based on the assumption that all sphingoids have 18 carbons. On the other hand, Hsu et al. (23) did structural studies of CER species in the SC. However, their structural analysis was restricted to a part of CERs that have shorter chain lengths in the sphingoid moieties.

The aim of this study was to characterize overall CER species in human SC. Normal-phase liquid chromatography (NPLC) connected to electrospray ionization-mass spectrometry (ESI-MS) was optimized for comprehensive profiling of diverse CERs in the SC, and overall CER species were visualized as 3D multi-mass chromatograms, followed by the structural analysis of the targeted peaks in the 3D chromatograms by NPLC-ESI-tandem mass spectrometry (MS/MS). Such analysis has also uncovered a new CER class consisting of α-hydroxy fatty acid and dihydrosphingosine moieties. Herein, we describe the results of identification of CERs in the SC, which are as many as 342 species.

MATERIALS AND METHODS

Nomenclature

Classes of CERs are termed according to previous reports (5, 24). Briefly, nonhydroxy fatty acid, α-hydroxy fatty acid, ester-linked nonhydroxy fatty acid, ω-hydroxy fatty acid, dihydrosphingosine, sphingosine, phytosphingosine, and 6-hydroxy-sphingosine moieties are designated as N, A, E, O, DS, S, P, and H, respectively. Based on this terminology, 12 classes of CERs (including classes not reported previously) are expressed as CER[NDS], CER[NS], CER[NP], CER[NH], CER[ADS], CER[AS], CER[AP], CER[AH], CER[EODS], CER[EOS], CER[EOP] and CER[EOH], as depicted in **Fig. 1**. For example, CER[NDS] corresponds to a CER class with N and DS. For each species, the number of fatty acid carbons and unsaturation (if present) is expressed following the letters of

Fatty acid \ Sphingoid	Non-hydroxy fatty acid [N]	α-hydroxy fatty acid [A]	Esterified ω-hydroxy fatty acid [EO]
Dihydrosphingosine [DS]	CER[NDS]	CER[ADS]	CER[EODS]
Sphingosine [S]	CER[NS]	CER[AS]	CER[EOS]
Phytosphingosine [P]	CER[NP]	CER[AP]	CER[EOP]
6-hydroxy sphingosine [H]	CER[NH]	CER[AH]	CER[EOH]

Fig. 1. Structures and nomenclature of ceramides (CERs) in human *stratum corneum* (SC).

N, A, E, or O in parentheses, and the number of sphingoid carbons is expressed following the letters DS, S, P, or H in parentheses, as represented in CER[E(18:2)O(30)H(20)] for a molecule consisting of ester-linked linoleic acid, ω-hydroxy triacontanoic acid, and C_{20} 6-hydroxy-sphingosine moieties.

Chemicals

Methanol, 2-propanol, chloroform, and n-hexane of HPLC grade from Kanto Reagents (Tokyo, Japan) were used to prepare extracted SC lipid solutions and mobile phases for NPLC. Ultra-pure water prepared using a Milli-Q purification system (Millipore; Bedford, MA) was used in all procedures. All other chemicals were of the highest analytical grade commercially available. Twelve authentic materials, CER[N(26)DS(20)], CER[N(26)S(20)], CER[N(26)P(20)], CER[N(26)H(20)], CER[A(26)DS(20)], CER[A(26)S(20)], CER[A(26)P(20)], CER[A(26)H(20)], CER[E(18:2)O(30)DS(20)], CER[E(18:2)O(30)S(20)], CER[E(18:2)O(30)P(20)], and CER[E(18:2)O(30)H(20)], were synthesized in our laboratory. Those authentic CERs were synthesized by coupling corresponding fatty acids and sphingoids in the presence of 1-ethyl-3-(3-diethylaminopropyl)carbodiimide hydrochloride, with 1-hydroxybenzotriazole as the coupling reagent (25). Constitutional fatty acids, except for hexacosanoic acid and linoleic acid, and sphingoids were prepared according to the literature (26–31). Each of the authentic CERs synthesized was purified with flash silica-gel column chromatography and/or recrystallization. Analyses by ^{1}H-NMR, ^{13}C-NMR, and infrared spectometry confirmed the structures (see supplementary Table I), and the purities were checked using TLC and LC-ultraviolet detection (>95%). Each authentic solution was prepared in a given molar solution. Individual authentic stock solutions (1 mM each) were prepared by dissolving accurate amounts of the authentic CERs in chloroform-methanol (1:1; v/v) and were stored at −4°C. When individual or mixed working authentic solutions were obtained, aliquots of the stock solutions were dried using a nitrogen stream, and the residues were diluted with n-hexane-2-propanol-formic acid (95:5:0.1; v/v/v) just prior to use.

Materials

The protocol was approved by the Ethical Committee of the Kao Corporation of Japan, based on recommendations from the Declaration of Helsinki. Tape-stripped SC specimens were collected from six healthy Japanese volunteers (three males 26 to 42 years old and three females 25 to 38 years old, who were enrolled in the study with informed consent) and were used to prepare extracted lipid materials, followed by the profiling of CERs using NPLC-ESI-MS. To obtain SC specimens, a polyphenylene sulfide film tape (Nichiban; Tokyo, Japan) with an area of 18 mm × 25 mm was pressed to the skin at the inner forearm and was then stripped. When 3 or 10 consecutive tapes were collected, they were pressed to the same region of the skin as the first one. The 3 or 10 tapes were immersed in methanol with sonication for 10 min. The lipid extracts were dried using a nitrogen stream and were then dissolved in chloroform-methanol (99.5:0.5; v/v). This lipid solution was applied to a Sep-Pak Vac RC silica cartridge (Waters; Milford, MA) that had been conditioned by chloroform-methanol (99.5:0.5; v/v), followed by solid-phase extraction with 10 ml chloroform-methanol (99.5:0.5; v/v) and 10 ml chloroform-methanol (99:5; v/v). The latter fraction, which contains the CERs, was dried using a nitrogen stream and then dissolved in n-hexane-2-propanol-formic acid (95:5:0.1; v/v/v). To identify CERs in the inner forearm SC, the extracted lipid samples obtained from a 34-year-old male and a 26-year-old female with 10 consecutive tapes were mixed and then subjected to NPLC-ESI-MS/MS. Amounts of lipid extracts from the 3 and 10 tapes were approximately 15 and 50 μg, respectively.

Analysis using NPLC-ESI-MS

An Agilent 1100 Series LC/MSD SL (single quadrupole) system equipped with an ESI source, ChemStation software, an 1100-well plate autosampler (Agilent Technologies; Palo Alto, CA), and an Inertsil SIL 100A-3, 1.5 mm i.d. × 150 mm column (GL Science; Tokyo, Japan) was used. In this LC/MSD system, an 1100 binary pump was connected to two mobile phases [A: n-hexane-2-propanol-formic acid (95:5:0.1; v/v/v); and B: n-hexane-2-propanol-50 mM ammonium formate aqueous solution (25:65:10; v/v/v)] with a flow rate of 0.1 ml/min. The mobile phases were consecutively programmed as follows: a linear gradient of A 100–90% (B 0–10%) between 0 and 3 min, a linear gradient of A 90–0% (B 10–100%) between 3 and 35 min, an isocratic elution of A 0% (B 100%) for 5 min, a linear gradient of A 0–100% (B 100–0%) between 40 and 50 min, and an isocratic elution of A 100% (B 0%) from 50 to 80 min for column equilibrium (a total run time of 80 min). The injection volume was 10 μl each of authentic solutions or extracted SC lipid solutions. The column temperature was maintained at 40°C. To enhance ionization of molecular-related ions derived from CERs in the mass spectrometer, 2.5 mM ammonium formate 2-propanol-methanol (50:50; v/v) at a flow rate of 0.1 ml/min was added to the mobile phase at the postcolumn position via a T-connector. Parameters for scan measurement of ESI using unit mass resolution mode was finally determined in the following settings: polarity, positive; heater temperature of nitrogen gas, 300°C; flow of heated dry nitrogen gas, 8.0 l/min; nebulizer gas pressure, 20 psi; capillary voltage, 3,500 V; fragmenter voltage, 150 V; scan range, 250–1,500 amu; scan time, 1.9 s/cycle.

Analysis using NPLC-ESI-MS/MS

A triple quadrupole API 4000 Q TRAP was equipped with an ESI (Turbo Ion Spray) source and Analyst version 1.0 software (Applied Biosystems; Foster City, CA), and was interfaced with an Agilent 1100 liquid chromatograph and a 1100-well plate autosampler (both from Agilent). The NPLC conditions were the same as those of the NPLC-ESI-MS. The positive- and negative-ion ESI-MS/MS measurements were employed, based on the Q_1 selection of the targeted precursor ions ([M + H]$^+$ or [M + H − H$_2$O]$^+$ for positive- and [M + HCOO]$^-$ for negative-ion mode) at the peaks detected and identified as CERs by NPLC-ESI-MS, followed by collision-induced dissociation in Q_2 and then followed by detection of the product ion spectra in Q_3. The positive-ion ESI-MS/MS conditions were performed together with unit mass resolution mode as follows: measurement mode, product ion scan; Q_1, 500–1,200 amu, 1,000 amu/s; Q_3, 200–600 amu, 1,000 amu/s; linear ion trap fill time, 15 ms; ion spray voltage, 5,500 V; ion source heater temperature, 600°C; ion source gases (N$_2$) for nebulizing, 50 psi; ion source gases (N$_2$) for drying solvent, 80 psi; curtain gas (N$_2$), 20 psi; declustering potential, 60 V; collision gas (N$_2$), 3×10^{-5} torr; collision energy, 40 V; collision exit energy, 10 V. In contrast, the negative-ion ESI-MS/MS conditions were as follows: Q_3, 200–600 amu, 1,000 amu/s; ion spray voltage, −4,500 V; declustering potential, −120 V for CER[EODS], CER[EOS], CER[EOP], and CER[EOH] and −60 V for the others; collision energy, −60 V. The other conditions were the same as those in the positive-ion ESI-MS/MS. Those parameters were determined based on preliminary experiments using authentic CERs to get the highest intensities of the targeted diagnostic ions.

RESULTS

### Optimization of NPLC-ESI-MS conditions

To analyze CERs in human SC using LC-MS, we decided to use NP and ESI modes in LC and MS, respectively, because the NP mode may enable the class separation of diverse CERs that have chain distributions both in the fatty acid and sphingoid moieties based on differences in their polarities, whereas the ESI mode seems to be the best for the LC-MS analysis of CERs, as demonstrated in many analytical studies (14, 15, 32–36).

First, the NPLC separation was optimized using 12 kinds of authentic materials, CER[N(26)DS(20)], CER[N(26)S(20)], CER[N(26)P(20)], CER[N(26)H(20)], CER[A(26)DS(20)], CER[A(26)S(20)], CER[A(26)P(20)], CER[A(26)H(20)], CER[E(18:2)O(30)DS(20)], CER[E(18:2)O(30)S(20)], CER[E(18:2)O(30)P(20)], and CER[E(18:2)O(30)H(20)]. By testing various combinations of high-polar silica-gel columns for LC (stationary phase) and low-polar solutions with n-hexane, alcohol, and acid/salt (mobile phase), we determined that a gradient elution system using mobile phase A (n-hexane-2-propanol-formic acid; 95:5:0.1; v/v/v) and mobile phase B (n-hexane-2-propanol-50 mM ammonium formate aqueous solution; 25:65:10;v/v/v) employed in a silica-gel column (Inertsil SIL 100A-3, 1.5 mm i.d. × 150 mm) provides better separation of the 12 authentic CERs.

Next, optimal conditions for the ESI-MS detection were examined. When a mixture of the mobile phase A:B = 50:50 (v/v) as a carrier was used at a flow rate of 0.1 ml/min under conditions of flow injection analysis, all authentic CERs yielded extremely less abundant intensities of their molecular-related ions. Because those results were thought to be caused by the low polarity of the carrier used (mobile phase A:B = 50:50), we attempted to enhance the ionization of the molecular-related ions by adding polar solvents and volatile acid/salt-containing solutions (a flow rate of 0.1 ml/min) to the carrier via a T-connector. As a result, although the addition of polar solvents and volatile acid-containing solutions barely improved the intensities of molecular-related ions, the addition of volatile salt-containing solutions drastically enhanced their intensities. Of all solutions tested, ammonium formate-containing 2-propanol-methanol (50:50; v/v) was the most effective (data not shown). Under such conditions, the positive-ion mode provided more-abundant intensities of the molecular-related ions, such as $[M + H - H_2O]^+$ for CER[N(26)H(20)], CER[A(26)H(20)], and CER[E(18:2)O(30)H(20)], and $[M + H]^+$ for the others, compared with $[M + HCOO]^-$ for all authentics in the negative-ion mode. Therefore, the combination of positive-ion ESI and postaddition of ammonium formate-containing 2-propanol-methanol solution following column separation was selected as the optimal condition for the detection of diverse CERs by MS. The concentration of ammonium formate was optimal at 2.5 mM in terms of signal to noise. MS parameters, such as heater temperature of nitrogen gas, flow of heated dry nitrogen gas, nebulizer gas pressure, capillary voltage, and fragmenter voltage, were optimized to achieve higher abundances of the targeted molecular-related ions for the 12 authentic CERs under positive-ion ESI-MS conditions (data not shown).

Fig. 2. shows a total ion chromatogram (TIC) of the 12 authentic CERs under optimized NPLC-ESI-MS conditions. All authentic CERs were detected as distinct peaks on the chromatograms and eluted within 20 min. Although chromatographic separations were not completely achieved between CER[E(18:2)O(30)S(20)] and CER[N(26)S(20)] or between CER[N(26)H(20)] and CER[A(26)P(20)], those CERs could be readily discriminated from each other by monitoring individual molecular-related ions in MS. The authentic CER[N(26)DS(20)] and CER[N(26)P(20)] (peaks #3 and #6 in Fig. 2, retention times of 7.2 and 12.4 min, respectively) predominantly yielded a proton adduct ion $[M + H]^+$ (m/z 708 and 724), in addition to some sodium adduct ion $[M + Na]^+$ (m/z 730 and 746) (see supplementary Fig. IA, C). Other authentic CER[A(26)DS(20)], CER[E(18:2)O(30)DS(20)], CER[A(26)P(20)], and CER[E(18:2)O(30)P(20)] had almost the same characteristics. The authentic CER[N(26)S(20)] (peak #4, 8.0 min) yielded a prominent $[M + H]^+$ (m/z 706), a less-abundant one, water loss ion $[M + H - H_2O]^+$ (m/z 688.6), and some $[M + Na]^+$ (m/z 728) (see supplementary Fig. IB), similar to authentic CER[A(26)S(20)] and CER[E(18:2)O(30)S(20)].
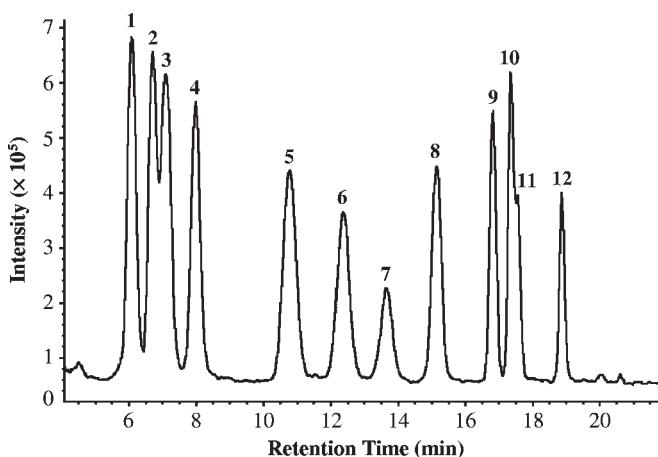
Fig. 2. Normal-phase liquid chromatography-electrospray ionization-mass spectrometry (NPLC-ESI-MS) total ion chromatogram (TIC) of 12 authentic CERs (2 μM each). Peaks: 1 = CER[E(18:2)O(30)DS(20)], 2 = CER[E(18:2)O(30)S(20)], 3 = CER[N(26)DS(20)], 4 = CER[N(26)S(20)], 5 = CER[E(18:2)O(30)P(20)], 6 = CER[N(26)P(20)], 7 = CER[A(26)DS(20)], 8 = CER[A(26)S(20)], 9 = CER[E(18:2)O(30)H(20)], 10 = CER[N(26)H(20)], 11 = CER[A(26)P(20)], 12 = CER[A(26)H(20)]. NPLC conditions: column, Inertsil SIL 100A-3 (1.5 mm i.d. × 150 mm); column temperature, 40°C; mobile phase A, n-hexane/2-propanol/formic acid, 95:5:0.1, by vol; mobile phase B, n-hexane/2-propanol/50 mM ammonium formate aqueous solution, 25:65:10, by vol; flow rate, 0.1 ml/min; gradient elution, see Materials and Methods; injection volume, 10 μl; postcolumn addition, 2.5 mM ammonium formate containing 2-propanol/methanol (50:50, by vol) at a flow rate of 0.1 ml/min. ESI-MS conditions: polarity, positive; heater temperature of nitrogen gas, 300°C; flow of heated dry nitrogen gas, 8.0 l/min; nebulizer gas pressure, 20 psi; capillary voltage, 3,500 V; fragmenter voltage, 150 V; scan range, 250–1,500 amu; scan time; 1.9 s/cycle.

In the mass spectrum of authentic CER[N(26)H(20)] (peak #10, 17.3 min), a predominant $[M + H - H_2O]^+$ (m/z 704.6) and some $[M + Na]^+$ (m/z 744.6) were observed (see supplementary Fig. ID). Those characteristics were also detected in mass spectra of CER[A(26)H(20)] and CER[E(18:2)O(30)H(20)]. This indicated that the mass spectral patterns are dependent on the types of sphingoid moieties, that is, the hydrophilic structures, under the less-polar mobile phase system. Thus, there seemed to be three types: *1)* DS- and P-containing CERs yielding abundant $[M + H]^+$; *2)* S-containing CERs yielding prominent $[M + H]^+$ and less-abundant $[M + H - H_2O]^+$; and *3)* H-containing CERs yielding only highly intensive $[M + H - H_2O]^+$. Taken together, for profiling CERs in the SC, it was determined that $[M + H]^+$ should be used for CER[NDS], CER[NS], CER[NP], CER[ADS], CER[AS], CER[AP], CER[EODS], CER[EOS], and CER[EOP], whereas $[M + H - H_2O]^+$ should be used for CER[NH], CER[AH], and CER[EOH].

Comprehensive profiling of CERs in human SC

The optimized NPLC-ESI-MS technique was then applied to the analysis of CERs in the SC. **Fig. 3.** shows the TIC for crude extracted lipids from three consecutive SC-stripped tapes of the inner forearm of a 34-year-old male. It was supposed that the CERs would elute at ~6 to 19 min under these chromatographic conditions, based on the retention times of authentic CERs, whereas large peaks eluting at ~20 min were judged to be contamination from the tapes used, because they appeared in blank analyses without any stripped SC. At an early stage of this study, on the basis of the characteristics of mass spectra of all peaks detected, we tried to observe overall CERs that are composed of diverse chain distributions both in fatty acid and sphingoid moieties, similar to a procedure reported by Farwanah et al. (22, 37). However, comprehensive observation was impossible, especially in the case of extremely low-abundance species, because m/z values corresponding to those species were often not found, due to the influence of high-content species.

To resolve this problem, we constructed 3D multi-mass chromatograms of the CERs, consisting of retention time (X-axis), m/z (Y-axis), and intensity (Z-axis), as presented in **Fig. 4**, which were constructed by extraction of 200 higher intensive ions in the range of retention times between 4 and 22 min from TIC of Fig. 3. The assignment of total carbons and unsaturation (if present) was performed as follows. *i)* We examined whether there were peaks that substantially coincided with retention times and m/z values of molecular-related ions derived from the 12 authentic CERs. *ii)* Other candidates, which differed from the identified CERs (i.e., authentic ones) at intervals of every carbon unit (14 as amu), were explored. In this survey, a regularly linear pattern was noted, in which retention times of CER species with higher molecular weights were slightly shorter than those with lower molecular weights under the NPLC conditions, in common with each class (Fig. 4). *iii)* As other possibilities, candidates that have differences of unsaturated degrees in N, A, E, or O moieties were also explored based on mass number gaps of 2 amu. *iv)* If there were no peaks corresponding to an authentic CER and no peaks were found in the neighborhood, a CER class was judged to be absent in the SC.

In the inner forearm SC of a 34-year-old male, the peaks were assigned as CER[NDS] (total carbons: C_{40-54}), CER[NS] (C_{40-54}), CER[NP] (C_{40-52}), CER[NH] (C_{36-50}), CER[ADS] (C_{38-46}), CER[AS] (C_{34-48}), CER[AP] (C_{34-50}), CER[AH] (C_{34-50}), CER[EOS] ($C_{65:2-72:2}$), CER[EOP] ($C_{66:2-70:2}$), and CER[EOH] ($C_{65:2-70:2}$) (Fig. 4). No species of CER[EODS] or with unsaturation in N, A, or O moieties were found. Similarly, we analyzed and assigned the CERs in the inner forearm SC of five other subjects (two males and three females). Consequently, the 3D multi-mass chromatograms and their assignment were almost the same as those of the 34-year-old male (data not shown). Thus, 11 CER classes were present in the SC tested; no species of CER[EODS] and none with unsaturated fatty acid moieties (except for E) were found. There were only differences in small peaks. A list of the commonly observed CERs in all subjects is shown in **Table 1**. This indicates that at least in the inner forearm SC of the six healthy subjects tested, N-containing CERs contain molecules with larger total carbons than do A-containing CERs. Also, EO-containing CERs had relatively narrow chain length distributions, compared with the other CERs.

Characteristics of product ion spectra of authentic CERs

The 12 authentic CERs were applied to NPLC-ESI-MS/MS to characterize their product ion spectra under the optimized NPLC separation conditions using the low polar mobile phases. Their positive product ion spectra were acquired, where $[M + H - H_2O]^+$ was used as a precursor ion for CER[N(26)H(20)], CER[A(26)H(20)], and CER[E(18:2)O(30)H(20)]. $[M + H]^+$ was used for the other authentic CERs, and their negative product ion spectra were acquired, where $[M + HCOO]^-$ was used
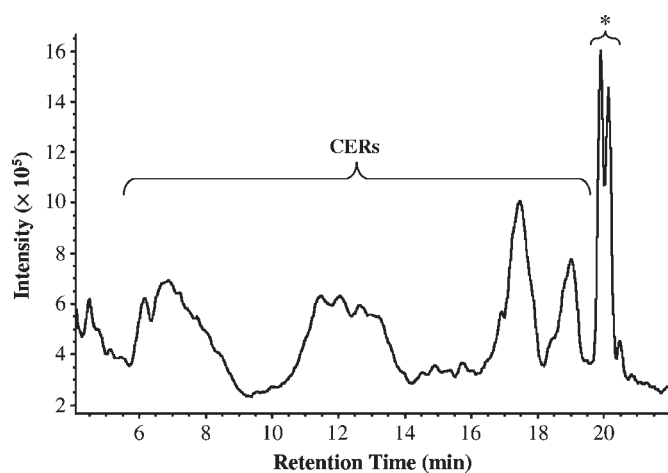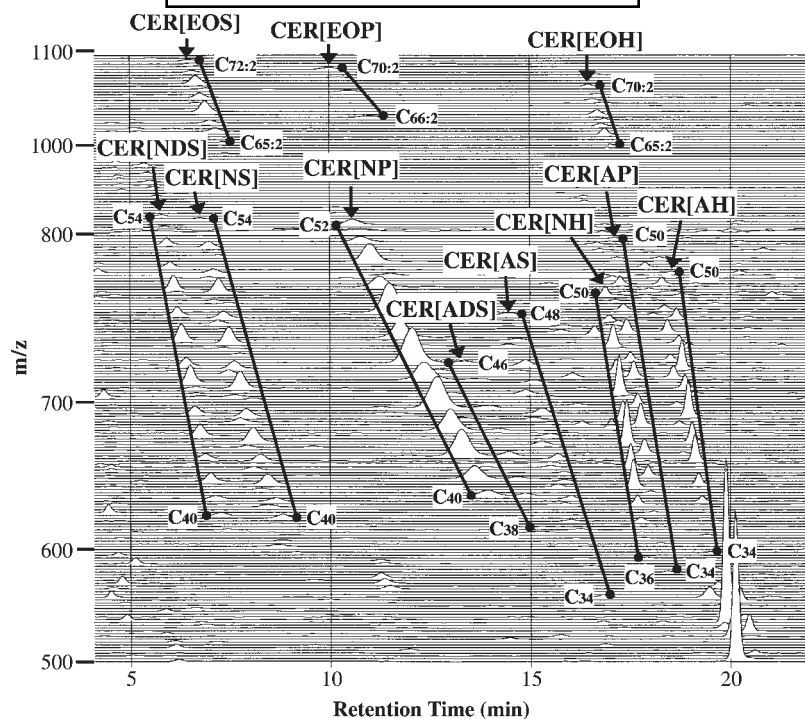

Fig. 3. NPLC-ESI-MS TIC of crude lipids extracted from three consecutive SC-stripped tapes (area 18 mm × 25 mm) from the inner forearm of a 34-year-old male. * Unknown substances caused by tapes used. For experimental conditions, see legend to Figure 2.

Fig. 4. 3D multi-mass chromatograms of CER species in the inner forearm SC using NPLC-ESI-MS. X-axis: retention time. Y-axis: *m/z*. Z-axis: intensity. The number of total carbons and unsaturation (if present) is expressed following the letter of C. The mass chromatograms were extracted from TIC of Figure 3.

as a precursor ion for all (see supplementary Fig. II). The product ions detected were assigned referring to previous studies on MS/MS structural analysis of CERs (15, 23, 38, 39). The nomenclature of the product ions followed the already-reported designation (36, 40).

CER[N(26)DS(20)] yielded the most prominent ion at *m/z* 312 and other ions at *m/z* 396, 294, and 330. The *m/z* 312 ion was assigned as that arising from the loss of one mole of water and fatty acyl group (O′), and the other ions, *m/z* 396, 294, and 330, were as U, O″, and O, respectively. In the product ion spectra of CER[N(26)S(20)], a predominant ion at *m/z* 292 (O″) and relatively weak ions at *m/z* 310 (O′), *m/z* 280 ([M + H − $C_{25}H_{50}CO$ − H_2O − HCHO]$^+$), and *m/z* 396 (U) were observed. CER[N(26)P (20)] had product ions at *m/z* 310 (O″), 328 (O′), 346 (O), 292 (O‴), and 396 (U) in the order of relative intensities. The MS/MS analysis of CER[N(26)H(20)] resulted in characteristic ions at *m/z* 308 (O″), 326 (O′), 290 (O‴), and 396 (U). The A-containing CERs had characteristics similar to those of the N-containing CERs, despite slight differences in the intensities, as follows: CER [A(26)DS(20)], O′ (*m/z* 312), U (412), O″ (294), and O (330); CER[A(26)S(20)], O″ (*m/z* 292), loss of HCHO from O′ (280), O′ (310), and U (412); CER[A(26)P(20)], O″ (*m/z* 310), O′ (328), O‴ (292), and U (412); CER[A (26)H(20)], O″ (*m/z* 308), U (412), 290 (O‴), and O′ (326), in the order of relative intensities. Also, the product ion spectra for the authentic EO-containing CERs are as follows: CER[E(18:2)O(30)DS(20)], O (*m/z* 330), O′ (312), and O″ (294); CER[E(18:2)O(30)S(20)], O″ (*m/z* 292), loss of

HCHO from O′ (280), and O′ (310); CER[E(18:2)O(30)P (20)], O″ (*m/z* 310), O (*m/z* 346), O′ (328), and O‴ (292); CER[E(18:2)O(30)H(20)], O″ (*m/z* 308), O′ (326), and O‴ (290), in the order of relative intensities.

In the negative-ion mode, CER[N(26)DS(20)] yielded the most prominent ion at *m/z* 420 and other ions at *m/z* 377, 267, 394, and 436, which were assigned to T, V, P, U, and S, respectively. CER[N(26)S(20)] showed product ions similar to those of CER[N(26)DS(20)], as detected in the most prominent ion, T (*m/z* 420), and others, P (265), V (377), U (394), and S (436) in the product ion spectra. In contrast, CER[N(26)P(20)] had a quite different product ion spectrum, in which the prominent ions were R (*m/z* 295), S (436), and U (394), whereas less-abundant P (283), T (420), V (377), and Q (253) were detected. CER[N(26)H(20)] yielded product ions T (420), U (394), S (436), P (263), and V (377), in the order of relative intensities. In the A-containing CERs, the most prominent ion, *m/z* 365 ([CHOC$_{24}$H$_{48}$]$^-$) was commonly observed. Other less-abundant ions, V (*m/z* 393), U (410), T (436), and P (267 for CER[A(26)DS(20)], 265 for CER[A(26)S(20)], 283 for CER[A(26)P(20)], and 263 for CER[A(26)H(20)]), were observed. CER[A(26)P(20)] also yielded R (*m/z* 295) and Q (253). In the product ion spectra of the EO-containing CERs, a prominent ion at *m/z* 279 was observed commonly. That ion was identified as [C$_{17}$H$_{31}$COO]$^-$. CER[E(18:2)O(30)DS(20)] and CER[E(18:2)O(30)H(20)] yielded other less-abundant ions, T (*m/z* 492) and U (466), whereas CER[E(18:2)O (30)S(20)] yielded T (492). On the other hand, in the
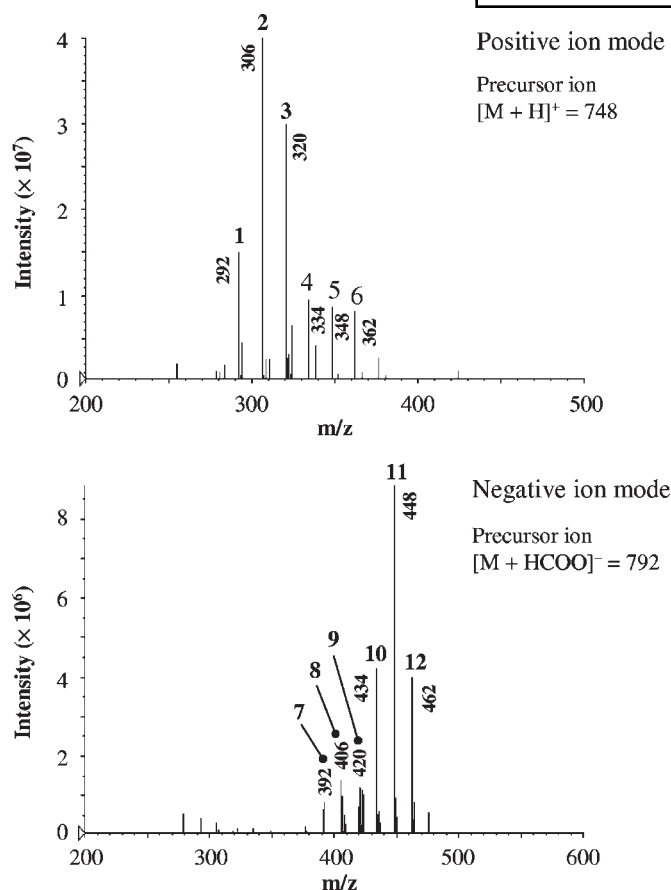
Fig. 5. NPLC-ESI-MS/MS product ion spectra of CER[NS] with 49 total carbons derived from the inner forearm SC. Assignment: 1, $[M + H - C_{28}H_{56}CO - 2H_2O]^+$ arising from CER[N(29)S(20)]; 2, $[M + H - C_{27}H_{54}CO - 2H_2O]^+$ from CER[N(28)S(21)]; 3, $[M + H - C_{26}H_{52}CO - 2H_2O]^+$ from CER[N(27)S(22)]; 4, $[M + H - C_{25}H_{50}CO - 2H_2O]^+$ from CER[N(26)S(23)]; 5, $[M + H - C_{24}H_{48}CO - 2H_2O]^+$ from CER[N(25)S(24)]; 6, $[M + H - C_{23}H_{46}CO - 2H_2O]^+$ from CER[N(24)S(25)]; 7, $[CH_2CHNHCOC_{23}H_{46}]^-$ from CER[N(24)S(25)]; 8, $[CH_2CHNHCOC_{24}H_{48}]^-$ from CER[N(25)S(24)]; 9, $[CH_2CHNHCOC_{25}H_{50}]^-$ from CER[N(26)S(23)]; 10, $[CH_2CHNHCOC_{26}H_{52}]^-$ from CER[N(27)S(22)]; 11, $[CH_2CHNHCOC_{27}H_{54}]^-$ from CER[N(28)S(21)]; 12, $[CH_2CHNHCOC_{28}H_{56}]^-$ from CER[N(29)S(20)].

product ion spectrum of CER[E(18:2)O(30)P(20)], ion m/z 504 was identified as $[CH_2C(CH_3)NHCOC_{29}H_{56}O]^-$, in addition to the ion U (466).

These results indicated that product ions obtained in the positive-ion mode can provide information on the number of carbons of sphingoid moieties and those obtained in the negative-ion mode can identify the number of carbons of fatty acid moieties. The total carbons of CERs in the inner forearm SC were assigned already, as shown in Fig. 4 and Table 1. To characterize combinations of fatty acid and sphingoid moieties for the CERs detected, we decided to use one of the prominent product ions for each of the positive- and negative-ion modes in NPLC-ESI-MS/MS, except for two product ions in the negative-ion mode for the identification of the EO-containing CERs, as shown in **Table 2**. Although identification using at least three

TABLE 1. Total carbons and unsaturation (if present) of CER species in human SC of the inner forearm, commonly observed in all six human subjects tested

Class	Total Carbons
CER[NDS]	40, 41, 42, 43, 44, 45, 46, 47, 48, 49, 50, 51, 52, 53, 54
CER[NS]	40, 41, 42, 43, 44, 45, 46, 47, 48, 49, 50, 51, 52
CER[NP]	40, 41, 42, 43, 44, 45, 46, 47, 48, 49, 50, 51, 52
CER[NH]	40, 41, 42, 43, 44, 45, 46, 47, 48, 49, 50
CER[ADS]	38, 40, 41, 42, 43, 44, 45, 46
CER[AS]	40, 41, 42, 43, 44, 45, 46, 47, 48
CER[AP]	38, 40, 41, 42, 43, 44, 45, 46, 48
CER[AH]	38, 39, 40, 41, 42, 43, 44, 45, 46, 47, 48
CER[EOS]	66:2, 67:2, 68:2, 69:2, 70:2
CER[EOP]	68:2, 69:2, 70:2
CER[EOH]	66:2, 67:2, 68:2, 69:2, 70:2

CER, ceramide; SC, *stratum corneum.*

diagnostic ions in a product ion spectrum would be desired for precise structural analysis using LC-MS/MS (16, 41), we decided to use only two diagnostic product ions (each derived from the positive and negative spectra) for N- or A-containing CERs, because we could detect prominent product ions derived from extremely low level CERs in actual crude lipid samples of SC but the corresponding less-abundant product ions could not be substantially detected due to the low detection sensitivity of the MS/MS scan analysis. However, in this study, the retention times greatly helped us to identify the individual CERs, in addition to the precursor/product ions arising from two different detection modes. As already described, the retention times obtained from this NPLC system were quite informative, because there was a regularly linear pattern for each of the CER classes commonly, under the optimized NPLC conditions (Fig. 4). Therefore, we supposed that reliable identification would be possible based on the evidence of the two diagnostic ions and the retention times.

Identification of overall CERs in human SC using NPLC-ESI-MS/MS

Figure 5 shows representative positive and negative product ion spectra of CER[NS] with 49 total carbons extracted from the inner forearm SC. In the positive product ion spectra, an ion at m/z 292 (ion #1 in Fig. 5) was assigned to $[M + H - C_{28}H_{56}CO - 2H_2O]^+$ according to the diagnostic ion of CER[NS] (Table 2). Because this indicated the presence of a nonhydroxy fatty acid with 29 carbons, it revealed that there is a CER[N(29)S(20)], together with consideration about the total carbons being 49. Similarly, the other positive ions were assigned, and CER[N(28)S(21)] (ion #2), CER[N(27)S(22)] (ion #3), CER[N(26)S(23)] (ion #4), CER[N(25)S(24)] (ion #5), and CER[N(24)S(25)] (ion #6) were identified. On the other hand, in negative product ion spectra, an ion at m/z 392 (ion #7) was assigned as $[CH_2CHNHCOC_{23}H_{46}]^-$ arising from CER[N(24)S(25)]. Also, the other negative ions were determined to come from CER[N(25)S(24)] (ion #8), CER[N(26)S(23)] (ion #9), CER[N(27)S(22)] (ion #10), CER[N(28)S(21)] (ion #11), and CER[N(29)S(20)] (ion #12). According to these procedures, all other

TABLE 2. Diagnostic product ions for structural analysis of CER species using NPLC-ESI-MS/MS

Class	Positive Product Ion	Negative Product Ion
CER[NDS][a,b]	$O' = [M + H - R_nCO - H_2O]^+$	$T = [CH_2CHNHCOR_n]^-$
CER[NS][a,b]	$O'' = [M + H - R_nCO - 2H_2O]^+$	$T = [CH_2CHNHCOR_n]^-$
CER[NP][a,b]	$O'' = [M + H - R_nCO - 2H_2O]^+$	$S = [CHOCH_2NHCOR_n]^-$
CER[NH][b,c]	$O'' = [M + H - R_nCO - 2H_2O]^+$	$T = [CH_2CHNHCOR_n]^-$
CER[ADS][a,b]	$O' = [M + H - R_aCH(OH)CO - H_2O]^+$	$[CHOR_a]^-$
CER[AS][a,b]	$O'' = [M + H - R_aCH(OH)CO - 2H_2O]^+$	$[CHOR_a]^-$
CER[AP][a,b]	$O'' = [M + H - R_aCH(OH)CO - 2H_2O]^+$	$[CHOR_a]^-$
CER[AH][b,c]	$O'' = [M + H - R_aCH(OH)CO - 2H_2O]^+$	$[CHOR_a]^-$
CER[EOS][a,b]	$O'' = [M + H - R_eCOOR_oCO - 2H_2O]^+$	$[R_eCOO]^-$
		$T = [CH_2CHNHCOR_oO]^-$
CER[EOP][a,b]	$O'' = [M + H - R_eCOOR_oCO - 2H_2O]^+$	$[R_eCOO]^-$
		$[CH_2C(CH_3)NHCOR_oO]^-$
CER[EOH][b,c]	$O'' = [M + H - R_eCOOR_oCO - 2H_2O]^+$	$[R_eCOO]^-$
		$T = [CH_2CHNHCOR_oO]^-$

NPLC-ESI-MS/MS, normal-phase liquid chromatography-electrospray ionization-tandem mass spectrometry. Alkyl/alkenyl chain: R_n for nonhydroxy fatty acid, R_a for α-hydroxy fatty acid, R_e for ester-linked fatty acid, R_o for ω-hydroxy fatty acid.
[a] Precursor ion, $[M + H]^+$.
[b] Precursor ion, $[M + HCOO]^-$.
[c] Precursor ion, $[M + H - H_2O]^+$.

peaks of the CERs assigned in the NPLC-ESI-MS analysis (Fig. 4, Table 2) were subjected to the structural analysis.

When peaks that were commonly observed in all six subjects (Table 1) were targeted, 342 species of CERs were identified; these include 75 types of CER[NDS], consisting of C_{16-30} N and C_{16-28} DS; 59 of CER[NS] of C_{16-30} N and C_{16-26} S; 39 of CER[NP] of C_{23-30} N and C_{16-26} P; 30 of CER[NH] of C_{23-30} N and C_{14-24} H; 28 of CER[ADS] of C_{16-27} A and C_{16-26} DS; 23 of CER[AS] of C_{22-27} A and C_{16-22} S; 20 of CER[AP] of C_{20-26} A and C_{16-22} P; 38 of CER[AH] of C_{20-30} A and C_{14-22} H; 10 of CER[EOS] of $C_{18:2}$ E C_{28-32} O and C_{18-22} S; 8 of CER[EOP] of $C_{18:2}$ E, C_{28-32} O, and C_{18-22} P; and 12 of CER[EOH] of $C_{18:2}$ E, C_{28-32} O, and C_{18-22} H (see supplementary Table II). Those CERs contained the great number of isobaric species that have identical molecular weights but different combinations of fatty acid and sphingoid moieties, as shown in the case of Fig. 5, which depicts six isobaric CER[NS] species having 49 total carbons.

DISCUSSION

In this study, as authentic materials, we used eight CERs having 46 total carbons that consist of 26 and 20 carbons in the fatty acid and sphingoid moieties, respectively, for N- or A-containing CERs, and four CERs having 68 total carbons consisting of 18, 30, and 20 carbons in E, O, and sphingoids, respectively, for EO-containing CERs. To comprehensively examine diverse CERs in the SC, it would be ideal to use various authentic materials of different chain lengths. However, it seemed impossible to synthesize all such materials when realistic tasks that would require very problematic and time-consuming labor were considered. Therefore, we adopted another strategy: we would use an authentic material representative of each CER class. As a result, in our preliminary survey on CERs in the SC, it was revealed that CER species having 46 total

carbons that consist of 26 and 20 carbons in the fatty acid and sphingoid moieties, respectively, seem to be commonly present and to be almost the center of the carbon length distributions in all N- or A-containing CER classes. Also, CER species having 68 total carbons, consisting of 18:2, 30, and 20 carbons in E, O, and sphingoid moieties, respectively, seemed to be common in all EO-containing CER classes except for CER[EODS]. Therefore, using 12 such authentic materials, we optimized NPLC-ESI-MS conditions and identified overall CER species present in the SC.

First, we optimized the NPLC conditions within 20 min, using a gradient elution system, which allowed the analysis of all CER species belonging to the 11 classes of CERs. One of the most ideal characteristics of this NPLC system is that different CER species belonging to the same class have regularly linear patterns in the chromatograms, in which CER species with higher molecular weights elute slightly earlier than those with lower molecular weights. This is extremely helpful in the practical analysis of CERs in SC specimens, because one can tentatively identify their total carbons using only their retention times and m/z values without a burdensome MS/MS analysis. Next, based on examinations of detection sensitivity, the post-column addition of a polar solvent, together with a volatile salt [2.5 mM ammonium formate-containing 2-propanol-methanol (50:50; v/v)] via a T-connection, is employed. This drastically enhances the intensities of molecular-related ions for all authentic CERs belonging to different classes. The drastic enhancement of detection leads to 3D visualization of CER profiles of the SC by their multi-mass chromatograms, consisting of retention time (X-axis), m/z (Y-axis), and intensity (Z-axis). Without such improvements in both separation and detection following such a 3D visualization, we would not have succeeded in the identification of overall CER species.

We had already developed a reverse-phase LC-MS method for CERs in hair (16). That method has an advantage in detection sensitivity compared with the NPLC-ESI-

MS method. However, that method is not appropriate currently to analyze overall CERs in the SC, because extremely hydrophobic CER species, such as EO-containing CERs, are not eluted under those reverse-phase conditions. To get peaks of the hydrophobic CERs, we could modify the analytical conditions by use of a more low-polar solvent as one of mobile phases in a reverse-phase gradient system. However, even if we got those peaks under reverse-phase conditions, the chromatogram would be too complicated to tentatively identify peaks of overall CERs due to complex separation based on both hydrophobic and hydrophilic degrees. In contrast to this, when the NPLC-ESI-MS method is used for the analysis of overall CERs in the SC, their tentative identification can be readily performed because the regularly linear patterns are available as mentioned above. Therefore, we believe that NPLC-ESI-MS is obviously superior to reverse-phase LC-MS from the standpoint of characterization of extremely diverse CERs in the SC, although detection sensitivity is lower.

The comprehensive profiling using NPLC-ESI-MS is followed by a comprehensive identification of diverse CERs in the SC by ESI-MS/MS analysis with both positive- and negative-ion modes under the NPLC conditions. Examination using authentic CERs reveals diagnostic product ions for each of the different CER classes, in which sphingoid (DS, S, P, and H)-related ions and fatty acid (N, A, E, and O)-related ions for each CER class are obtained in positive- and negative-ion modes, respectively. According to those diagnostic product ions, the NPLC-ESI-MS/MS analysis results in the identification of 342 species of CERs, consisting of a large number of isobaric species within the 11 CER classes, which demonstrates the presence of CER[ADS] composed of C_{16-27}-containing A and C_{16-26}-containing DS. Because until now there have been no reports describing the presence of CER[ADS] in the SC, we have discovered a new class of CER[ADS] in the SC for the first time. It should be kept in mind that analytically targeted peaks were restricted to those commonly observed in all six subjects tested, and that more than 342 CER species would have been identified in the SC if the analytical conditions had had a higher detection sensitivity. However, it seems that the major species of CERs have all been identified. We observed no differences in the 3D chromatographic patterns of CER species providing relatively large peaks between individuals tested, although there were differences in those providing relatively small peaks (data not shown). In conclusion, we successfully achieved comprehensive identification of CERs, which number as many as at least 342 species, under the optimized NPLC-ESI-MS/MS conditions.

Here, we consider novel aspects regarding the structures of CER species in the SC. This study clarified combinations of constitutional fatty acids and sphingoids that comprise 342 distinct CER species. Although a few reports have described combinations of fatty acid and sphingoid moieties in CER species (19, 22, 23), our study is substantially the first report of the precise identification of overall CER species in the SC, because the previous reports were based on the assumption that all sphingoids have 18 carbons (19,

22), or were restricted to CERs that have shorter chain lengths in their sphingoid moieties (23). The validity of our results can be estimated by comparison with a previous report by Wertz et al. (42), who used GC with derivatizing techniques and then analyzed both the fatty acid and sphingoid moieties that had been obtained from the hydrolysis of each of the isolated CER classes. The number of carbons of N or A moiety in CER[NDS], CER[NS], CER[NP], CER[AS], and CER[ADS] identified in this study is roughly consistent with that report (42), despite slight differences. In the E moiety of CER[EOS], we detected only linoleic acid, whereas Wertz et al. (42) found that linoleic acid was the most predominant, although palmitic acid, stearic acid, and oleic acid were also present. As for the number of carbons of the DS, S, or P moiety, although our results are nearly the same as those of the earlier report (42), our study reveals a slightly greater number of carbons, presented as C_{16-28} DS in CER[NDS] and C_{16-26} S in CER[NS], compared with the previous result, C_{16-22} in both classes (42). Those slight differences might be derived from distinct origins, including inter-individual variations, or from other factors, such as experimental artifacts during the preparative procedures or by GC separation performance. Nonetheless, the differences are only slight, and we believe that our identification results are close to the previous report (42). Some scientists may believe that C_{18}-containing sphingoids are predominant in the SC (19, 22), but our study demonstrates that there are many CER species with long-chain (more than C_{18})-containing sphingoids in the SC.

When compared with CERs in other human cells/tissues, including hair, it is evident that CERs in the SC are characterized by the diversity of CER classes, as is generally known. In addition, this study indicates that another characteristic of CERs in the SC is that the species have longer chain lengths, especially in sphingoids, than do those of other cells/tissues, including hair. This is exemplified by the facts that CER[NS] in the SC is composed of C_{16-30} N and C_{16-26} S moieties, whereas CER[NS] in other cells/tissues (except for hair) is composed of C_{16-26} N and C_{18} S (43, 44), and that CER[NDS] in the SC is composed of C_{16-30} N and C_{16-28} DS, whereas CER[NDS] in hair is composed of C_{14-30} N and C_{16-20} DS (16). This characteristic may be necessary to maintaining the barrier function of human skin, possibly because CER species with longer chain lengths seem to be appropriate for preventing water from diffusing from the SC to the outside, or for preventing chemicals from penetrating from the outside to the SC. Regarding the comparison between CERs in the SC and hair, there are similarities and differences. The similar characteristics are the large number of odd carbons-containing CERs, some of which are assumed to have branched chains either in the fatty acid or the sphingoid moiety in human hair (16). The presence of odd carbons-containing CERs in the SC is in agreement with the previous study by Wertz et al. (42). As is generally known, human sebum has odd carbons-containing fatty acids with branched carbon skeletons (45). Therefore, the odd carbons-containing CERs in the SC might have branched

chains. This possibility should be clarified in the future by further investigations, together with synthesis of authentic CERs containing branched fatty acids and/or branched sphingoids. On the other hand, one different characteristic is that CERs in the SC have no unsaturated fatty acid moieties except for E (linoleic acid), whereas hair contains many CER species with unsaturated ones (16). Despite different and unknown characteristics, CERs in the SC are relatively similar to hair CERs, compared with other cells/tissues. This may be due to the anatomical and developmental similarities of human skin and hair.

Currently known de novo pathways for diverse CERs in human SC are arranged as follows: *1*) production of 3-ketosphinganine from palmitoyl-CoA and L-serine by serine palmitoyltransferase (46); *2*) production of dihydrosphingosine from 3-ketosphinganine by 3-ketosphinganine (3-ketodihydrosphingosine) reductase (46); *3*) production of α-hydroxy fatty acid from nonhydroxy fatty acid by 2-hydroxylase, designated as FA2H (47); *4*) production of CER[NDS] and CER[ADS] from dihydrosphingosine, and nonhydroxy fatty acid and α-hydroxy fatty acid (precisely their CoA forms) by ceramide synthase 1-6 (48); *5*) production of CER[NS] and CER[AS] from CER[NDS] and CER[ADS] by dihydroceramide desaturase, designated as DEGS1 (49); and *6*) production of CER[NP] and CER[AP] from CER[NDS] and CER[ADS] by hydroxylase, designated as DEGS2 (50). To our knowledge, the biosynthetic pathways for EO-containing and/or H-containing CERs are unknown at present. However, it can be assumed that the biosynthetic pathway of H-containing CERs would be similar to those of S- or P-containing CERs by unidentified enzymes, that is, H-containing CERs might be produced from DS-containing CERs. Taken together with our results on the identification of overall CER species in the SC, these pathways lead us to the interesting notion. Thus, according to the above pathway, C_{18}-containing DS would be preferentially produced in human epidermis, followed by the occurrence of CER species with C_{18}-containing sphingoids. However, we identified many species with long-chain (more than C18)-containing sphingoids in the SC. This phenomenon is of considerable interest from the viewpoint of the biosynthesis of CERs in human skin. In addition, there are differences in chain length distributions of both fatty acid and sphingoid moieties among CER[NDS], CER[NS], CER[NP], and CER[NH], or among CER[ADS], CER[AS], CER[AP], and CER[AH], although CER[NS], CER[NP], and CER[NH], or CER[AS], CER[AP], and CER[AH] may be biosynthesized from their identical precursors, CER[NDS] or CER[ADS], respectively. This might suggest the chain-dependent selectivity of DEGS1, DEGS2, and unidentified H-containing CER-related enzyme(s). Further study will be required to clarify phenomena that might be related to the reasons that CER species with such extremely diverse chain length distributions are present in the SC.

In conclusion, we have structurally analyzed overall CER species in human SC using a newly constructed NPLC-ESI-MS/MS technique, followed by 3D multi-mass chromatograms. This has revealed that there are at least 342 species within 11 classes in the SC. Those CER species include a new class, CER[ADS], long-chain (more than C_{18})-containing sphingoid moieties, and a great number of isobaric species. These novel results will contribute not only to future research on the physiochemical roles of CERs at the species level in the SC but also to lipidomics approaches to CERs (and CER-related lipids) in the skin. Our next project will be to design another method for providing comprehensively quantitative levels of the 342 CER species; methods exist for the quantification of specific CER species but not for the comprehensive quantification of as many as the 342 CER species present in the SC. Such a quantitative method could be of further use in the study of the physicochemical relationships between the CER species and the various types of SC (different ages, sexes, regions, skin conditions, and so on), or in research into the lipidomics of CERs in the skin, such as clarification of the physiological roles of specific CER(s) during keratinization and of the de novo biosynthesis of diverse CER species of different chain lengths. That method should be also highly sensitive, because small amounts of crude lipids obtained from only one SC-stripped tape can be applied. That is because if such a highly sensitive method is acquired, we may even characterize depth profiles of overall CER species within the SC by analysis of each of the tapes consecutively stripped at the same SC regions.∎

REFERENCES

1. Fishbein, J. D., R. T. Dobrowsky, A. Bielawska, S. Garrett, and Y. A. Hannun. 1993. Ceramide-mediated growth inhibition and CAPP are conserved in *Saccharomyces cerevisiae*. *J. Biol. Chem.* **268:** 9244–9261.
2. Hannun, Y. A. 1996. Functions of ceramide in coordinating cellular responses to stress. *Science.* **274:** 1855–1859.
3. Pettus, B. J., C. E. Chalfant, and Y. A. Hannun. 2002. Ceramide in apoptosis: an overview and current perspectives. *Biochim. Biophys. Acta.* **1585:** 114–125.
4. Venable, M. E., L. M. Webb-Froehlich, E. F. Sloan, and J. E. Thomley. 2006. Shift in sphingolipid metabolism leads to an accumulation of ceramide in senescence. *Mech. Ageing Dev.* **127:** 473–480.
5. Robson, K. J., M. E. Stewart, S. Michelsen, N. D. Lazo, and D. T. Downing. 1994. 6-Hydroxy-4-sphingenine in human epidermal ceramides. *J. Lipid Res.* **35:** 2060–2068.
6. Elias, P. M. 1983. Epidermal lipids, barrier, function, and desquamation. *J. Invest. Dermatol.* **80 (Suppl.):** 44–49.
7. Imokawa, G., S. Akasaki, M. Hattori, and N. Yoshizuka. 1986. Selective recovery of deranged water-holding properties by stratum corneum lipids. *J. Invest. Dermatol.* **87:** 758–761.
8. Imokawa, G., S. Akasaki, Y. Minematsu, and M. Kawai. 1989. Importance of intercellular lipids in water-retention properties of the stratum corneum: induction and recovery study of surfactant dry skin. *Arch. Dermatol. Res.* **281:** 45–51.
9. Holleran, W. M., K. R. Feingold, M. Q. Man, W. N. Gao, J. M. Lee, and P. M. Elias. 1991. Regulation of epidermal sphingolipid synthesis by permeability barrier function. *J. Lipid Res.* **32:** 1151–1158.
10. Hamanaka, S., S. Nakazawa, M. Yamanaka, Y. Uchida, and F. Otsuka.

2005. Glucosylceramide accumulates preferentially in lamella bodies in differentiated keratinocytes. *Br. J. Dermatol.* **152:** 426–434.

11. Thomas, R. L., C. M. Matsko, M. T. Lotze, and A. A. Amoscato. 1999. Mass spectrometric identification of increased C$_{16}$ ceramide levels during apoptosis. *J. Biol. Chem.* **274:** 30580–30588.

12. Fujiwaki, T., S. Yamaguchi, K. Sukegawa, and T. Taketomi. 1999. Application of delayed extraction matrix-assisted laser desorption ionization time-of-flight mass spectrometry for analysis of sphingolipids in tissues from sphingolipidosis patients. *J. Chromatogr. B Analyt. Technol. Biomed. Life Sci.* **731:** 45–52.

13. Pettus, B. J., M. Baes, M. Busman, Y. A. Hannun, and P. P. van Veldhoven. 2004. Mass spectrometric analysis of ceramide perturbations in brain and fibroblasts of mice and human patients with peroxisomal disorders. *Rapid Commun. Mass Spectrom.* **18:** 1569–1574.

14. Liebisch, G., W. Drobnik, M. Reil, B. Trümbach, R. Arneche, B. Olgemöller, A. Roscher, and G. Schmitz. 1999. Quantitative measurement of different ceramide species from crude cellular extracts by electrospray ionization tandem mass spectrometry (ESI-MS/MS). *J. Lipid Res.* **40:** 1539–1546.

15. Han, X. 2002. Characterization and direct quantitation of ceramide molecular species from lipid extracts of biological samples by electrospray ionization tandem mass spectrometry. *Anal. Biochem.* **302:** 199–212.

16. Masukawa, Y., H. Tsujimura, and H. Narita. 2006. Liquid chromatography-mass spectrometry for comprehensive profiling of ceramide molecules in human hair. *J. Lipid Res.* **47:** 1559–1571.

17. Imokawa, G., A. Abe, K. Jin, Y. Higaki, M. Kawashima, and A. Hidano. 1991. Decreased level of ceramides in stratum corneum of atopic dermatitis: an etiologic factor in atopic dry skin? *J. Invest. Dermatol.* **96:** 523–526.

18. Long, S. A., P. W. Wertz, J. S. Strauss, and D. T. Downing. 1985. Human stratum corneum polar lipids and desquamation. *Arch. Dermatol. Res.* **277:** 284–287.

19. Vietzke, J. P., O. Brandt, D. Abeck, C. Rapp, M. Strassner, V. Schreiner, and U. Hintze. 2001. Comparative investigation of human stratum corneum ceramides. *Lipids.* **36:** 299–304.

20. Ponec, M., A. Weerheim, P. Lankhorst, and P. W. Wertz. 2003. New acylceramide in native and reconstructed epidermis. *J. Invest. Dermatol.* **120:** 581–588.

21. Wertz, P. W., K. C. Madison, and D. T. Downing. 1987. Covalently bound lipids of human stratum corneum. *J. Invest. Dermatol.* **92:** 109–111.

22. Farwanah, H., J. Wohlrab, R. H. H. Neubert, and K. Raith. 2005. Profiling of human stratum corneum ceramides by means of normal phase LC/APCI-MS. *Anal. Bioanal. Chem.* **383:** 632–637.

23. Hsu, F. F., J. Turk, M. E. Stewart, and D. T. Downing. 2002. Structural studies on ceramides as lithiated dissociation by low energy collisional-activated dissociation tandem mass spectrometry with electrospray ionization. *J. Am. Soc. Mass Spectrom.* **13:** 680–695.

24. Motta, S., M. Monti, S. Sesana, R. Caputo, S. Carelli, and R. Ghidoni. 1993. Ceramide composition of the psoriatic scale. *Biochim. Biophys. Acta.* **1182:** 147–151.

25. Mori, K., and K. Uenishi. 1994. A new synthesis of symbioramide, a Ca^{++}-ATPase activator from Symbiodinium sp. *Liebigs Ann. Chem.* **1994:** 41–48.

26. Mori, K., and Y. Funaki. 1985. Synthesis of (4E, 8E, 2S, 3R, 2'R)-N-2'-hydroxyhexadecanoyl-9-methyl-4,8-sphigadienine, the ceramide portion of the fruiting-inducing cerebroside in a basidiomycete schizophyllum commune and its (2R, 3S)-isomer. *Tetrahedron.* **41:** 2369–2377.

27. Mori, K., and H. Matsuda. 1991. Synthesis of (2S, 3R, 4E)-1-O-(β-D-glucopyranosyl)-N-[30'-(linoleoyloxy)triacontanoyl]-4-icosasphingenine, a new esterified cerebroside from human and pig epidermis. *Liebigs Ann. Chem.* **1991:** 529–535.

28. Imashiro, R., O. Sakurai, T. Yamashita, and H. Horikawa. 1998. A short and efficient synthesis of phytosphingosines using asymmetric dihydroxylation. *Tetrahedron.* **54:** 10657–10670.

29. Lee, J. M., H. S. Lim, and S. K. Chung. 2002. A short and efficient streoselective synthesis of all four diastereomers of sphingosine. *Tetrahedron Asymmetry.* **13:** 343–347.

30. Chun, J., H. S. Byun, and R. Bittman. 2003. First asymmetric synthesis of 6-hydroxy-4-sphingenine-containing ceramides. Use of chiral propargylic alcohols to prepare a liquid found in human skin. *J. Org. Chem.* **68:** 348–354.

31. Mori, K., and Y. Masuda. 2003. Synthesis and stereochemistry of ceramide B, (2S, 3R, 4E, 6R)-N-(30-hydroxytriacintanoyl)-6-hydroxy-4-sphingenine, a new ceramide in human epidermis. *Tetrahedron Lett.* **44:** 9197–9200.

32. Mano, N., Y. Oda, K. Yamada, N. Asakawa, and K. Katayama. 1997. Simultaneous quantitative determination method for sphingolipid metabolites by liquid chromatography/ionspray ionization tandem mass spectrometry. *Anal. Biochem.* **244:** 291–300.

33. Gu, M., J. L. Kerwin, J. D. Watts, and R. Aebersold. 1997. Ceramide profiling of complex lipid mixtures by electrospray ionization mass spectrometry. *Anal. Biochem.* **244:** 347–356.

34. Vietzke, J. P., M. Strassner, and U. Hintze. 1999. Separation and identification of ceramides in the human stratum corneum by high-performance liquid chromatography coupled with electrospray ionization mass spectrometry and electrospray multiple-stage mass spectrometry profiling. *Chromatographia.* **50:** 15–20.

35. Fillet, M., J. C. van Heugen, A. C. Servais, J. de Graeve, and J. Crommen. 2002. Separation, identification and quantitation of ceramides in human cancer cells by liquid chromatography-electrospray ionization tandem mass spectrometry. *J. Chromatogr. A.* **949:** 225–233.

36. Lee, M. H., G. H. Lee, and J. S. Yoo. 2003. Analysis of ceramides in cosmetics by reversed-phase liquid chromatography/electrospray ionization mass spectrometry with collision-induced dissociation. *Rapid Commun. Mass Spectrom.* **17:** 64–75.

37. Farwanah, H., K. Raith, R. H. H. Neubert, and J. Wohlrab. 2005. Ceramide profiles of the uninvolved skin in atopic dermatitis and psoriasis are comparable to those of healthy skin. *Arch. Dermatol. Res.* **296:** 514–521.

38. Raith, K., and R. H. H. Neubert. 1998. Structural studies on ceramides by electrospray tandem mass spectrometry. *Rapid Commun. Mass Spectrom.* **12:** 935–938.

39. Hsu, F. F., and J. Turk. 2002. Characterization of ceramides by low energy collisional-activated dissociation tandem mass spectrometry with negative-ion electrospray ionization. *J. Am. Soc. Mass Spectrom.* **13:** 558–570.

40. Ann, Q., and J. Adams. 1993. Structure-specific collision-induced fragmentations of ceramides cationized with alkali-metal ions. *Anal. Chem.* **65:** 7–13.

41. Matsui, Y., S. Nakamura, N. Kondou, Y. Takasu, R. Ochiai, and Y. Masukawa. 2007. Liquid chromatography-electrospray ionization-tandem mass spectrometry for simultaneous analysis of chlorogenic acids and their metabolites in human plasma. *J. Chromatogr. B Analyt. Technol. Biomed. Life Sci.* **858:** 96–105.

42. Wertz, P. W., D. C. Swartzendruber, K. C. Madison, and D. T. Downing. 1987. Composition and morphology of epidermal cyst lipids. *J. Invest. Dermatol.* **89:** 419–425.

43. Yamada, Y., K. Kajiwara, M. Yano, E. Kishida, Y. Masuzawa, and S. Kojo. 2001. Increase of ceramides and its inhibition by catalase during chemically induced apoptosis of HL-60 cells determined by electrospray ionization tandem mass spectrometry. *Biochim. Biophys. Acta.* **1532:** 115–120.

44. Drobnik, W., G. Liebisch, X. D. Fröhlich, T. Glück, P. Vogel, G. Rothe, and G. Schmitz. 2003. Plasma ceramide and lysophosphatidylcholine inversely correlate with mortality in sepsis patients. *J. Lipid Res.* **44:** 754–761.

45. Nicolaides, N. 1974. Skin lipids: their biochemical uniqueness. *Science.* **186:** 19–26.

46. Merrill, A. H., and C. C. Sweeley. 1996. Sphingolipids: metabolism and cell signaling. *In* Biochemistry of Lipids, Lipoproteins and Membranes. D. E. Vance and J. E. Vance, editors. Elsevier, New York. 309–339.

47. Alderson, N. L., B. M. Rembiesa, M. D. Walla, A. Bielawska, J. Bielawski, and H. Hama. 2004. The human FA2H gene encodes a fatty acid 2-hydroxylase. *J. Biol. Chem.* **279:** 48562–48568.

48. Zheng, W., J. Kollmeyer, H. Symolon, A. Momin, E. Munter, E. Wang, S. Kelly, J. C. Allegood, Y. Liu, Q. Peng, et al. 2006. Ceramides and other bioactive sphingolipid backbones in health and disease: lipidomic analysis, metabolism and roles in membrane structure, dynamics, signaling and autophagy. *Biochim. Biophys. Acta.* **1758:** 1864–1884.

49. Kraveka, J. M., L. Li, Z. M. Szulc, J. Bielawski, B. Ogretmen, Y. A. Hannun, L. M. Obeid, and A. Bielawska. 2007. Involvement of dihydroceramide desaturase in cell cycle progression in human neuroblastoma cells. *J. Biol. Chem.* **282:** 16718–16728.

50. Mizutani, Y., A. Kihara, and Y. Igarashi. 2004. Identification of the human sphingolipid C4-hydroxylase, hDES2, and its up-regulation during keratinocyte differentiation. *FEBS Lett.* **563:** 93–97.